

# Charmed quark component of the photon wave function

V.V. Anisovich, L.G. Dakhno, V.N. Markov, V.A. Nikonov and A.V. Sarantsev

27.10.2004

## Abstract

We determine the  $c\bar{c}$  component of the photon wave function on the basis of  
 (i) the data on the transitions  $e^+e^- \rightarrow J/\psi(3096), \psi(3686), \psi(4040), \psi(4415)$ ,  
 (ii) partial widths of the two-photon decays  $\eta_{c0}(2979), \chi_{c0}(3415), \chi_{c2}(3556) \rightarrow \gamma\gamma$ , and  
 (iii) wave functions of the charmonium states obtained by solving the Bethe-Salpeter equation for the  $c\bar{c}$  system. Using the obtained  $c\bar{c}$  component of the photon wave function we calculate the  $\gamma\gamma$  decay partial widths for radial excitation  $2S$  state,  $\eta_{c0}(3594) \rightarrow \gamma\gamma$ , and  $2P$  states  $\chi_{c0}(3849), \chi_{c2}(3950) \rightarrow \gamma\gamma$ .

## 1 Introduction

There is a number of processes that can be sensibly treated by introducing the  $c\bar{c}$  component of the photon wave function. First, it is the production of charmonium in the two-photon transitions such as  $\gamma^*\gamma^* \rightarrow c\bar{c}$ -mesons, production of  $\psi$ -mesons in the  $e^+e^-$ -annihilation and production of charmonia in photon-nucleon collisions,  $\gamma^*p \rightarrow c\bar{c}$ -meson +  $X$ . In the present paper, we determine the  $c\bar{c}$ -component of photon wave function, or the transition vertex  $\gamma \rightarrow c\bar{c}$ , following the method developed in [1,2], where quark-antiquark components were found for the transitions  $\gamma \rightarrow u\bar{u}, d\bar{d}, s\bar{s}$ .

The method of introducing quark-antiquark photon wave function may be clearly illustrated by considering the  $c\bar{c}$ -meson  $\rightarrow \gamma\gamma$  decay. Dealing with the time-ordered processes, that is necessary in the dispersion relation approach or light-cone variable technique, the  $c\bar{c}$ -meson  $\rightarrow \gamma\gamma$  decay is a two-step process: first, the emission of photon by quark (Fig. 1a) or antiquark (Fig. 1b) and, second, subsequent annihilation  $c\bar{c} \rightarrow \gamma$ .

In Refs. [1, 2], the triangle diagrams of Figs. 1a,b were treated in terms of double dispersion relation representation. The double spectral integral cuttings of the diagram in Fig. 1a are shown on Fig. 1c. In the diagram of Fig. 1c, on the left from the first cutting, there is the transition vertex of charmonium,  $G_{charmonium}(s)$ , decaying into  $c\bar{c}$  pair, where  $s$  is the quark invariant energy squared. In light-cone variables

$$s = \frac{m_c^2 + k_\perp^2}{x(1-x)}, \quad (1)$$

where  $m_c$  is the mass of  $c$ -quark and  $(x, \mathbf{k}_\perp)$  are the characteristics of one of the quarks (fraction of the momentum along the  $z$ -axis and transverse component). In the dispersion integral, the left-hand cutting leads to the factor  $G_{charmonium}/(s - M_{charmonium}^2)$ , where  $M_{charmonium}$  is the charmonium mass, this factor being the wave function of the initial  $c\bar{c}$ -meson:

$$\frac{G_{charmonium}(s)}{s - M_{charmonium}^2} = \Psi_{charmonium}(s) . \quad (2)$$

Likewise, the right-hand cut in Fig. 1c, by describing the transition  $c\bar{c} \rightarrow \gamma$ , gives us the factor:

$$\frac{1}{s'} e_c , \quad (3)$$

where  $s'$  is the invariant energy square of quarks in the final state and  $e_c$  is the  $c$ -quark charge.

When we deal with the transition  $c\bar{c} \rightarrow \gamma$ , the interaction of quarks should be specially taken into consideration. The quarks may interact both in the initial (Fig. 2a) and final (Fig. 2b) states. In fact, the interaction of quarks in the initial state has been accounted for by Eq. (2), because the vertex function  $G_{charmonium}$  (or wave function  $\Psi_{charmonium}$ ) is the solution of Bethe-Salpeter equation — diagrammatically, this equation is shown in Fig. 3a. As to quark interaction in the final state, it should be particularly taken into account in addition to the point-like interaction (3). The diagram shown in Fig. 3b stands for the description of quark interaction in the transition  $c\bar{c} \rightarrow \gamma$ , and we approximate it with the sum of the  $\psi$ -mesons pole terms, see Fig. 3c. Accordingly, the factor related to the right-hand cut of Fig. 1c is written as follows:

$$\frac{G_{\gamma \rightarrow c\bar{c}}(s')}{s'} e_c , \quad (4)$$

where the vertex function  $G_{\gamma \rightarrow c\bar{c}}(s')$  at  $s' \sim 4m_c^2$  is a superposition of vertices of the  $S$ -wave  $\psi$ -mesons (see Fig. 3c):

$$G_{\gamma \rightarrow c\bar{c}}(s) \simeq \sum_n C_n G_{\psi(nS)}(s) , \quad s \sim 4m_c^2 . \quad (5)$$

Here  $n$  is the radial quantum number of  $\psi$ -meson and  $C_n$ 's are numerical coefficients — their definition is the task of this paper. At large  $s$ , the vertex  $c\bar{c} \rightarrow \gamma$  is a point-like one:

$$G_{\gamma \rightarrow c\bar{c}}(s) \simeq 1 \quad \text{at} \quad s > s_0 . \quad (6)$$

The parameter  $s_0$  can be determined using the data on  $e^+e^-$ -annihilation into hadrons: it is defined by the energy range, where the ratio  $R(s) = \sigma(e^+e^- \rightarrow \text{hadrons})/\sigma(e^+e^- \rightarrow \mu^+\mu^-)$  reaches a constant-behaviour regime above the threshold of the charm production,  $R(s) \simeq 10/3$ . The data support the value  $s_0 \sim (10 - 15) \text{ GeV}^2$  [3].

Therefore, to describe the transition  $c\bar{c} \rightarrow \gamma$  we may introduce a characteristics, which, similarly to (2), may be called the charmed quark component of photon wave function:

$$\frac{G_{\gamma \rightarrow c\bar{c}}(s)}{s - q^2} = \Psi_{\gamma(q^2) \rightarrow c\bar{c}}(s) , \quad (7)$$

here  $q$  is the photon four-momentum. Let us emphasize that such a wave function is determined at  $s \gtrsim 4m_c^2$ .

There exists a reaction which is directly related to the photon wave function. This is the transition  $e^+e^- \rightarrow \psi(nS)$ , see Fig. 4: here the loop diagram is defined by the convolution of meson wave function and the vertex  $\gamma \rightarrow c\bar{c}$ :  $\Psi_{nS} \otimes G_{\gamma \rightarrow c\bar{c}}$ .

Dealing with the  $c\bar{c}$  interaction in the transition  $\gamma \rightarrow c\bar{c}$ , we take into consideration the  $S$ -wave  $\psi$ -mesons only, while the contribution of mesons dominated by the  $D$ -wave such as  $\psi(3770)$  and  $\psi(4160)$ , is neglected. The error coming from such a neglect can be evaluated by comparing the  $\psi$ -meson production cross sections for  $S$ - and  $D$ -wave states in the  $e^+e^-$ -annihilation: it is of the order of 10%. The  $D$ -wave admixture into the low-lying  $1^{--}$ -mesons is also small: it is of the order of 1% for  $J/\psi(1S)$  and  $\psi(2S)$  [4].

We are performing calculations of two- and three-point loop diagram in the spectral integration technique. All the equations used, up to trivial substitutions of quark masses and charges, were obtained in [5]. Because of that, in this paper we present final expressions only accompanied by necessary comments and references.

The main difference between calculations for  $\gamma \rightarrow c\bar{c}$  and those for  $\gamma \rightarrow u\bar{u}, d\bar{d}, s\bar{s}$  carried out in [1, 2] consists in our regard towards quark wave functions. In [1, 2], we used phenomenological quark wave functions for  $\pi^0, \eta, \eta'$ , while for light vector mesons ( $\rho, \omega, \phi$ ) we assumed the quark wave functions to be similar to analogous pseudoscalar-meson wave functions, with whom they form the lowest 36-plet in terms of SU(6)-symmetry. But here, when reconstructing the wave function for the transition  $\gamma \rightarrow c\bar{c}$ , we have applied the charmonium wave functions found out from the solution of Bethe-Salpeter equation [4].

It was a long history of calculation of charmonium states, and now there is a rich collection of results obtained in the framework of the nonrelativistic approaches [6, 7, 8, 9] as well as in different variants of the Bethe-Salpeter equation [10, 11, 12, 13], see also references therein. However, one should bear in mind that in calculations related to quark-antiquark systems, one focuses as a rule on the description of levels (or masses) of the system. Had the potential or its relativistic analogue been known, the Bethe-Salpeter equation would undoubtedly provide us with both levels and wave functions. But the problem is that in fact our knowledge about the quark-quark interaction in the soft region is rather poor. Therefore, in the reconstruction of quark-antiquark levels one can obtain a variety of wave functions. Within the spectral integration technique used here, we see that unambiguous determination of interaction is possible in the simultaneous description of both levels and wave functions, see discussion in Section 2.6.3 of [5]. Because of that, by describing the  $c\bar{c}$  system, we have used in [4] as an input both the known levels and known values of radiative transitions  $(c\bar{c})_{in} \rightarrow \gamma + (c\bar{c})_{out}$ . These radiative transitions are rather sensitive to wave functions, thence a comparatively good description of radiation transitions in [4] allows us to believe that the wave functions of lowest  $c\bar{c}$  states are determined reliably too.

The paper is organized as follows. In Section 2 we present briefly the information about the spectral-integration Bethe-Salpeter equation, in the framework of which the description

of the  $c\bar{c}$  systems was performed in [4]. In Section 2 of the present article we also give the charmonium wave functions obtained at the determination of  $G_{\gamma \rightarrow c\bar{c}}$ . In Section 3 we write down the formulae for the transition amplitudes  $e^+e^- \rightarrow \psi$  and  $\eta_{c0}, \chi_{c0}, \chi_{c2} \rightarrow \gamma\gamma$ , which are used in the fit, and present the results for the photon wave function. Brief summary is given in Conclusion.

## 2 Charmonium wave functions

The spectral integral equation for quark-antiquark wave function, which can be conventionally called as the Bethe-Salpeter equation, is written for a system with the total momentum  $J$ , angular momentum  $L$ , quark-antiquark spin  $S$  and radial number  $n$ . For the  $c\bar{c}$  system it reads:

$$\begin{aligned} & \left( s - M_{charmonium}^2 \right) \widehat{\Psi}_{(n)\mu_1 \dots \mu_J}^{(S,L,J)}(k_\perp) = \\ & = \int_{4m_c^2}^{\infty} \frac{ds'}{\pi} d\Phi_2(P'; k'_1, k'_2) \widehat{V}(s, s', (k_\perp k'_\perp)) (\hat{k}'_1 + m_c) \widehat{\Psi}_{(n)\mu_1 \dots \mu_J}^{(S,L,J)}(k'_\perp) (-\hat{k}'_2 + m_c) . \end{aligned} \quad (8)$$

Here the quarks are mass-on-shell,  $k_1^2 = k_1'^2 = k_2^2 = k_2'^2 = m_c^2$ , and the phase space factor in the intermediate state is determined as follows:

$$d\Phi_2(P'; k'_1, k'_2) = \frac{1}{2} \frac{d^3 k'_1}{(2\pi)^3 2k'_{10}} \frac{d^3 k'_2}{(2\pi)^3 2k'_{20}} (2\pi)^4 \delta^{(4)}(P' - k'_1 - k'_2) . \quad (9)$$

We use the following notations:

$$\begin{aligned} k_\perp &= \frac{1}{2}(k_1 - k_2) , \quad P = k_1 + k_2 , \quad k'_\perp = \frac{1}{2}(k'_1 - k'_2) , \quad P' = k'_1 + k'_2 , \\ P^2 &= s , \quad P'^2 = s' , \quad g_{\mu\nu}^\perp = g_{\mu\nu} - \frac{P_\mu P_\nu}{s} , \quad g_{\mu\nu}'^\perp = g_{\mu\nu} - \frac{P'_\mu P'_\nu}{s'} , \end{aligned} \quad (10)$$

so one can write  $k_\mu^\perp = k_\nu g_{\nu\mu}^\perp$  and  $k'_\mu^\perp = k'_\nu g_{\nu\mu}'^\perp$ . In the centre-of-mass system, the integration can be re-written as

$$\int_{4m_c^2}^{\infty} \frac{ds'}{\pi} d\Phi_2(P'; k'_1, k'_2) \longrightarrow \int \frac{d^3 k'}{(2\pi)^3 k'_0} , \quad (11)$$

where  $k'$  is the momentum of one of the quarks. The wave function reads:

$$\widehat{\Psi}_{(n)\mu_1 \dots \mu_J}^{(S,L,J)}(k_\perp) = Q_{\mu_1 \dots \mu_J}^{(S,L,J)}(k_\perp) \psi_n^{(S,L,J)}(k_\perp^2) . \quad (12)$$

Here  $Q_{\mu_1 \dots \mu_J}^{(S,L,J)}(k_\perp)$  is the moment operator for fermion-antifermion system [14] defined as follows:

$$\begin{aligned} Q_{\mu_1 \mu_2 \dots \mu_J}^{(0,J,J)}(k_\perp) &= i\gamma_5 X_{\mu_1 \dots \mu_J}^{(J)}(k_\perp) , \\ Q_{\mu_1 \dots \mu_J}^{(1,J+1,J)}(k_\perp) &= \gamma_\alpha^\perp X_{\mu_1 \dots \mu_J \alpha}^{(J+1)}(k_\perp) , \\ Q_{\mu_1 \dots \mu_J}^{(1,J,J)}(k_\perp) &= \frac{1}{\sqrt{s}} \varepsilon_{\alpha\nu_1\nu_2\nu_3} \gamma_\alpha^\perp P_{\nu_1} Z_{\nu_2\mu_1 \dots \mu_J, \nu_3}^{(J)}(k_\perp) , \\ Q_{\mu_1 \dots \mu_J}^{(1,J-1,J)}(k_\perp) &= \gamma_\alpha^\perp Z_{\mu_1 \dots \mu_J, \alpha}^{(J-1)}(k_\perp) , \end{aligned} \quad (13)$$

where

$$\begin{aligned}
X_{\mu_1 \dots \mu_J}^{(J)}(k_\perp) &= \frac{(2J-1)!!}{J!} \left[ k_{\mu_1}^\perp k_{\mu_2}^\perp k_{\mu_3}^\perp k_{\mu_4}^\perp \dots k_{\mu_J}^\perp - \right. \\
&- \frac{k_\perp^2}{2J-1} \left( g_{\mu_1 \mu_2}^\perp k_{\mu_3}^\perp k_{\mu_4}^\perp \dots k_{\mu_J}^\perp + g_{\mu_1 \mu_3}^\perp k_{\mu_2}^\perp k_{\mu_4}^\perp \dots k_{\mu_J}^\perp + \dots \right) + \\
&+ \frac{k_\perp^4}{(2J-1)(2J-3)} \left( g_{\mu_1 \mu_2}^\perp g_{\mu_3 \mu_4}^\perp k_{\mu_5}^\perp k_{\mu_6}^\perp \dots k_{\mu_J}^\perp + \right. \\
&\left. + g_{\mu_1 \mu_2}^\perp g_{\mu_3 \mu_5}^\perp k_{\mu_4}^\perp k_{\mu_6}^\perp \dots k_{\mu_J}^\perp + \dots \right) + \dots \left. \right], \tag{14}
\end{aligned}$$

$$\begin{aligned}
Z_{\mu_1 \dots \mu_J, \alpha}^{(J-1)}(k_\perp) &= \frac{2J-1}{L^2} \left( \sum_{i=1}^J X_{\mu_1 \dots \mu_{i-1} \mu_{i+1} \dots \mu_J}^{(J-1)}(k_\perp) g_{\mu_i \alpha}^\perp - \right. \\
&\left. - \frac{2}{2J-1} \sum_{\substack{i,j=1 \\ i < j}}^J g_{\mu_i \mu_j}^\perp X_{\mu_1 \dots \mu_{i-1} \mu_{i+1} \dots \mu_{j-1} \mu_{j+1} \dots \mu_J}^{(J-1)}(k_\perp) \right).
\end{aligned}$$

The interaction block can be expanded in a series in a full set of the  $t$ -channel operators:

$$\widehat{V}(s, s', (k_\perp k'_\perp)) = \sum_I V_I(s, s', (k_\perp k'_\perp)) \widehat{O}_I \otimes \widehat{O}_I, \tag{15}$$

$$\widehat{O}_I = \mathbf{I}, \quad \gamma_\mu, \quad i\sigma_{\mu\nu}, \quad i\gamma_\mu \gamma_5, \quad \gamma_5.$$

The Bethe-Salpeter equation (8) is written in the momentum representation, it was solved in [4] in the momentum representation as well. Equation (8) allows one to use as an interaction the instantaneous approximation or to take into account retardation effects. In the instantaneous approximation one has

$$\widehat{V}(s, s', (k_\perp k'_\perp)) \longrightarrow \widehat{V}(t_\perp), \quad t_\perp = (k_{1\perp} - k'_{1\perp})_\mu (-k_{2\perp} + k'_{2\perp})_\mu \tag{16}$$

The retardation effects are taken into account, when the momentum transferred squared  $t$  in the interaction block depends on the time components of quark momenta (for more detail see Section 2.5 of [5] and the discussion in [13, 20, 22, 23]):

$$\widehat{V}(s, s', (k_\perp k'_\perp)) \longrightarrow \widehat{V}(t), \quad t = (k_1 - k'_1)_\mu (-k_2 + k'_2)_\mu. \tag{17}$$

It turned out that for the fit of the  $c\bar{c}$  states we need only two interaction blocks with the following  $t$ -dependence:

$$\begin{aligned}
I_0(t) &= \frac{8\pi\mu}{(\mu^2 - t)^2}, \\
I_1(t) &= 8\pi \left( \frac{4\mu^2}{(\mu^2 - t)^3} - \frac{1}{(\mu^2 - t)^2} \right). \tag{18}
\end{aligned}$$

It also occurred that the results of the fit depended weakly on whether the  $t$ - or  $t_\perp$ -dependence was used in (18). Because of that, for the sake of simplicity, we present below the results obtained in the instantaneous approximation substituting  $t \rightarrow t_\perp$  in (18).

Traditionally, the interaction of heavy quarks in the instantaneous approximation is presented in terms of the potential  $V(r)$ . The form of the potential can be obtained with the Fourier transform of (18) in the centre-of-mass system. Thus we have

$$\begin{aligned} t_\perp &= -(\vec{k} - \vec{k}')^2 = -\vec{q}^2, \\ I_c^{(N)}(r, \mu) &= \int \frac{d^3q}{(2\pi)^3} e^{-i\vec{q}\vec{r}} I_N(t_\perp), \end{aligned} \quad (19)$$

that gives

$$I_c^{(0)}(r, \mu) = e^{-\mu r}, \quad I_c^{(1)}(r, \mu) = r e^{-\mu r}. \quad (20)$$

The potential used in [4] had the form

$$V(r) = a + b r + c e^{-\mu r}, \quad (21)$$

where the constant and linear (confinement) terms read:

$$\begin{aligned} a &\rightarrow a I_c^{(0)}(r, \mu_{constant} \rightarrow 0), \\ br &\rightarrow b I_c^{(1)}(r, \mu_{linear} \rightarrow 0). \end{aligned} \quad (22)$$

The limits  $\mu_{constant}, \mu_{linear} \rightarrow 0$  mean that in the fitting procedure the parameters  $\mu_{constant}$  and  $\mu_{linear}$  are chosen to be small enough, of the order of 1–10 MeV. It was checked that the solution for the considered states ( $n \leq 6$ ) was stable when changing  $\mu_{constant}$  and  $\mu_{linear}$  in this interval, 1–10 MeV.

In [4], charmonium wave functions were fitted in the following form:

$$\Psi_{charmonium}^{(n)}(s) = e^{-\beta k^2} \sum_{i=1}^9 c_i^{(n)} k^{i-1}. \quad (23)$$

Recall that  $k^2$  is the relative quark momentum squared,  $s = 4m_c^2 + 4k^2$ , and  $n$  is the radial quantum number;  $\beta = 1 \text{ GeV}^{-2}$  for all  $c\bar{c}$  states.

Two solutions with two types of the  $t$ -channel exchanges were used:

$$\begin{aligned} \text{Solution I} &: \quad \text{I} \otimes \text{I}, \quad \gamma_\mu \otimes \gamma_\mu, \quad \gamma_5 \otimes \gamma_5, \\ \text{Solution II} &: \quad \text{I} \otimes \text{I}, \quad \gamma_\mu \otimes \gamma_\mu. \end{aligned}$$

Table 1 demonstrates the obtained values of the potential parameters ( $a, b, c, \mu$ ) in Solutions I and II. In all solutions we put  $m_c = 1.25 \text{ GeV}$ .

The measured masses of the  $c\bar{c}$ -states and the results of the fit for  $n = 1, 2, 3, 4, 5, 6$  are displayed in Table 2.

Table 1: Parameters of the potential (in GeV units)

Type of interaction ( $\widehat{O}_I \otimes \widehat{O}_I$ )	Solution	$a$	$b$	$c$	$\mu$
Scalar ( $I \otimes I$ )	I	-1.527	0.170	1.013	0.201
	II	-1.417	0.158	0.883	0.201
Vector ( $\gamma_\mu \otimes \gamma_\mu$ )	I	-1.539	0	2.133	0.401
	II	-1.540	0	2.130	0.401
Pseudoscalar ( $\gamma_5 \otimes \gamma_5$ )	I	-3.000	0	0	0.201
	II	0	0	0	-

Figure 5 shows the radiative decay transitions, which were included into fitting procedure in [4]. One can see the calculated numbers for partial widths and experimental values with errors used in the fit: the 20%-accuracy was accepted for the transitions  $\psi(2S) \rightarrow \gamma\chi_{cJ}(1P)$  and 30%-one for  $\chi_{cJ}(1P) \rightarrow \gamma\psi(1S)$  (note that slightly smaller errors were obtained in the overall fit of Ref. [15]).

The wave function parameters  $c_i^{(n)}$  determined in (23) are presented in Table 3 for Solutions I and II. Correspondingly, in Figs. 6 and 7 we demonstrate the wave functions for  $\psi(nS)$  and  $\eta_c, \chi_{c0}, \chi_{c1}, \chi_{c2}$ . Comparing the wave functions depicted in Figs. 6 and 7, one can clearly see that Solutions I and II differ insignificantly. We have carried out our calculations with two variants of the interaction in order to make clear that the description of  $c\bar{c}$  system does not require a variety of the  $t$ -channel exchanges and inclusion of all the versions given by Eq. (15) would only result in the absence of convergence in fitting procedure. In particular, the considered example of two sorts of interactions demonstrate that the  $c\bar{c}$  system does not require instanton-induced forces, which were needed for treating the mass splitting of  $\pi, \eta, \eta'$  [16].

### 3 Determination of the $c\bar{c}$ component of the photon wave function

The vertex function of the transition  $\gamma \rightarrow c\bar{c}$  is represented with the following formula:

$$G_{\gamma \rightarrow c\bar{c}}(s) = \sum_{n=1}^6 C_n G_{\psi(nS)}(s) + \frac{1}{1 + \exp[(-\beta_\gamma(s - s_0))]} , \quad (24)$$

where  $G_{\psi(nS)}(s) = \Psi_{\psi(nS)}(s)(s - M_{\psi(nS)}^2)$  and  $M_{\psi(nS)}$  and  $\Psi_{\psi(nS)}(s)$  are given in Tables 2 and 3;  $C_n, \beta_\gamma$  and  $s_0$  are the parameters to be determined.

Table 2: Measured masses and results of the fit for Solutions I and II (in GeV units). Bold-faced numbers stand for masses which have been used in fitting procedure [4].

n	$\psi(nS)$		$\eta_c(nS)$		$\chi_{c0}(nP)$		$\chi_{c1}(nP)$		$\chi_{c2}(nP)$	
	data	fit	data	fit	data	fit	data	fit	data	fit
1	<b>3.096</b>	3.1022	<b>2.979</b>	2.9776	<b>3.415</b>	3.3933	<b>3.510</b>	3.4962	<b>3.556</b>	3.5676
2	<b>3.686</b>	3.6737	<b>3.594</b>	3.6246		3.8485		3.9002		3.9495
3	4.040	4.0565		4.0225		4.1812		4.2514		4.3046
4	4.415	4.3960		4.3678		4.5569		4.6709		4.8250
5		4.8465		4.8233		5.1185		5.1886		5.4758
6		5.4448		5.4242		5.7510		5.8404		6.2197
1	<b>3.096</b>	3.1023	<b>2.979</b>	2.9772	<b>3.415</b>	3.3958	<b>3.510</b>	3.4979	<b>3.556</b>	3.5687
2	<b>3.686</b>	3.6721	<b>3.594</b>	3.6238		3.8447		3.8957		3.9434
3	4.040	4.0470		4.0139		4.1705		4.2406		4.2976
4	4.415	4.3801		4.3527		4.5488		4.6605		4.8188
5		4.8322		4.8090		5.1123		5.1820		5.4669
6		5.4336		5.4135		5.7460		5.8379		6.1986

Table 3: Constants  $c_i^{(n)}$  (in GeV units) for the wave functions of Eq.(23) in Solutions I, II

$i$	$J/\psi(1S)$	$\psi(2S)$	$\psi(3S)$	$\psi(4S)$	$\eta_c(1S)$	$\eta_c(2S)$	$\chi_{c0}(1P)$	$\chi_{c0}(2P)$	$\chi_{c2}(1P)$	$\chi_{c2}(2P)$
1	8.15	-18.87	43.70	-68.75	-7.064	-17.72	27.17	131.60	-45.15	-144.38
2	3.01	9.16	-271.18	682.41	0.08171	4.60	-12.77	-480.42	59.15	569.17
3	-48.02	266.00	465.83	-2356.65	20.748	247.04	-100.08	539.03	141.47	-587.98
4	76.13	-729.46	-92.87	3873.67	-14.849	-653.28	181.19	-23.55	-432.83	-315.11
5	-49.16	871.28	-504.13	-3421.29	-22.992	770.56	-120.56	-442.03	481.62	1126.02
6	9.17	-566.22	587.76	1688.66	41.115	-500.42	23.01	410.77	-286.31	-978.20
7	4.81	208.18	-286.06	-452.00	-25.682	185.63	11.05	-172.89	96.19	413.89
8	-2.65	-40.78	66.18	57.34	7.413	-37.01	-6.04	36.23	-17.21	-87.74
9	0.3712	3.320	-5.948	-2.183	-0.8335	3.094	0.8269	-3.081	1.274	7.454
1	8.14	-19.41	45.87	-69.8	-7.061	-18.16	27.79	137.91	-46.32	-151.59
2	2.86	12.56	-295.78	705.5	0.29980	7.16	-15.64	-520.67	64.72	624.91
3	-47.50	260.19	559.16	-2482.2	19.754	243.34	-95.29	633.58	132.65	-753.22
4	75.58	-729.85	-261.10	4172.7	-13.001	-655.51	177.81	-131.97	-428.51	-59.52
5	-48.97	882.00	-338.96	-3793.5	-24.954	781.02	-120.21	-377.56	484.48	895.03
6	9.20	-578.49	494.77	1949.0	42.396	-511.22	23.98	393.18	-290.87	-851.60
7	4.76	214.44	-256.26	-554.9	-26.199	190.89	10.43	-172.64	98.47	372.46
8	-2.63	-42.31	61.177	78.7	7.527	-38.26	-5.88	37.11	-17.73	-80.30
9	0.371	3.468	-5.6097	-4.01	-0.84433	3.212	0.8118	-3.211	1.320	6.891



### 3.1 Decay $\psi(nS) \rightarrow e^+e^-$

Partial width for the decay  $\psi(nS) \rightarrow e^+e^-$  reads:

$$\Gamma(\psi(nS) \rightarrow e^+e^-) = \frac{\pi\alpha^2}{M_{\psi(nS)}^5} \sqrt{\frac{M_{\psi(nS)}^2 - 4\mu_e^2}{M_{\psi(nS)}^2}} \left( \frac{8}{3}\mu_e^2 + \frac{4}{3}M_{\psi(nS)}^2 \right) |F_{\psi(nS) \rightarrow e^+e^-}(0)|^2, \quad (25)$$

where  $\alpha = e^2/4\pi = 1/137$ ,  $\mu_e$  is the electron mass, and  $M_{\psi(nS)}$  is the charmonium mass. The transition amplitude  $F_{\psi(nS) \rightarrow e^+e^-}(0)$ , being determined by the process of Fig. 4, see [1], is equal to:

$$F_{\psi(nS) \rightarrow e^+e^-}(0) = \frac{2}{3} \sqrt{N_c} \int_{4m_c^2}^{\infty} \frac{ds}{16\pi^2} \Psi_{\psi(nS)}(s) G_{\gamma \rightarrow c\bar{c}}(s) \sqrt{1 - \frac{4m_c^2}{s}} \left( \frac{8}{3}m_c^2 + \frac{4}{3}s \right). \quad (26)$$

The wave function in (26) is normalized as follows:

$$1 = \int_{4m_c^2}^{\infty} \frac{ds}{16\pi^2} \Psi_{\psi(nS)}^2(s) \sqrt{1 - \frac{4m_c^2}{s}} \left( \frac{8}{3}m_c^2 + \frac{4}{3}s \right). \quad (27)$$

The coefficients  $c_i^{(n)}$  given in Table 3 construct the wave functions obeying this normalization constraint.

### 3.2 Decay $\eta_c(nP) \rightarrow \gamma\gamma$

Partial width for the decay  $\eta_c \rightarrow \gamma\gamma$  reads:

$$\Gamma(\eta_c \rightarrow \gamma\gamma) = \frac{\pi}{4} \alpha^2 M_{\eta_c}^3 |F_{\eta_c \rightarrow \gamma\gamma}(0)|^2. \quad (28)$$

The transition amplitude is determined by the processes of Figs. 1a,b; it is equal to [1, 4, 17]:

$$F_{\eta_c(nP) \rightarrow \gamma\gamma}(0) = \frac{8}{9} \sqrt{N_c} m_c \int_{4m_c^2}^{\infty} \frac{ds}{2\pi^2} \Psi_{\eta_c(nP)}(s) \Psi_{\gamma \rightarrow c\bar{c}}(s) \ln \frac{\sqrt{s} + \sqrt{s - 4m_c^2}}{\sqrt{s} - \sqrt{s - 4m_c^2}}, \quad (29)$$

where  $N_c = 3$ . Recall that  $\Psi_{\gamma \rightarrow c\bar{c}}(s) = G_{\gamma \rightarrow c\bar{c}}(s)/s$ .

Normalization condition for pseudoscalar charmonium wave functions is as follows:

$$1 = \int_{4m_c^2}^{\infty} \frac{ds}{8\pi^2} \Psi_{\eta_c(nP)}^2(s) \sqrt{1 - \frac{4m_c^2}{s}} s. \quad (30)$$

Coefficients presented in Table 3 give us  $\Psi_{\eta_c(nP)}(s)$  obeying (30).

### 3.3 Decay $\chi_{c0}(nP) \rightarrow \gamma\gamma$

Partial width of the decay  $\chi_{c0} \rightarrow \gamma\gamma$  is equal to

$$\Gamma(\chi_{c0} \rightarrow \gamma\gamma) = \frac{\pi\alpha^2}{M_{\chi_{c0}}} |F_{\chi_{c0} \rightarrow \gamma\gamma}(0)|^2, \quad (31)$$

with the quark transition amplitude (Figs. 1a,b) determined as follows [17, 18]:

$$F_{\chi_{c0}(nP) \rightarrow \gamma\gamma}(0) = \frac{8}{9} \sqrt{N_c} m_c \int_{4m_c^2}^{\infty} \frac{ds}{4\pi^2} \Psi_{\chi_{c0}(nP)}(s) \Psi_{\gamma \rightarrow c\bar{c}}(s) \left( \sqrt{s(s-4m_c^2)} - 2m_c^2 \ln \frac{\sqrt{s} + \sqrt{s-4m_c^2}}{\sqrt{s} - \sqrt{s-4m_c^2}} \right). \quad (32)$$

Normalization condition for scalar charmonium wave function reads:

$$1 = \int_{4m_c^2}^{\infty} \frac{ds}{8\pi^2} \Psi_{\chi_{c0}(nP)}^2(s) \sqrt{1 - \frac{4m_c^2}{s}} (s - 4m_c^2) m_c^2. \quad (33)$$

### 3.4 Decay $\chi_{c2}(nP) \rightarrow \gamma\gamma$

Partial width  $\chi_{c2} \rightarrow \gamma\gamma$  is defined by two transition amplitudes:

$$\Gamma(\chi_{c2} \rightarrow \gamma\gamma) = \frac{4}{5} \frac{\pi\alpha^2}{M_{\chi_{c2}}} \left( \frac{1}{6} |F_{\chi_{c2} \rightarrow \gamma\gamma}^{(0)}(0)|^2 + |F_{\chi_{c2} \rightarrow \gamma\gamma}^{(2)}(0)|^2 \right), \quad (34)$$

which are determined by the processes of Figs. 1a,b [17, 19] and for the  $P$ -wave quark-antiquark states they read: equal to:

$$F_{\chi_{c2}(nP) \rightarrow \gamma\gamma}^{(H)}(0) = \frac{8}{9} \sqrt{N_c} \int_{4m_c^2}^{\infty} \frac{ds}{16\pi^2} \Psi_{\chi_{c2}(nP)}(s) \Psi_{\gamma \rightarrow c\bar{c}}(s) I^{(H)}(s). \quad (35)$$

Here

$$I^{(0)}(s) = -2\sqrt{s(s-4m_c^2)} (12m_c^2 + s) + 4m_c^2 (4m_c^2 + 3s) \ln \frac{s + \sqrt{s(s-4m_c^2)}}{s - \sqrt{s(s-4m_c^2)}}, \quad (36)$$

$$I^{(2)}(s) = \frac{4\sqrt{s(s-4m_c^2)}}{3} (5m_c^2 + s) - 4m_c^2 (2m_c^2 + s) \ln \frac{s + \sqrt{s(s-4m_c^2)}}{s - \sqrt{s(s-4m_c^2)}}.$$

Normalization condition for the  $P$ -wave tensor  $c\bar{c}$  system it is:

$$1 = \int_{4m_c^2}^{\infty} \frac{ds}{16\pi^2} \Psi_{\chi_{c2}(nP)}^2(s) \frac{8}{15} \sqrt{1 - \frac{4m_c^2}{s}} (8m_c^2 + 3s)(s - 4m_c^2). \quad (37)$$

### 3.5 The results of the fit

By fitting the reactions involving the transition  $\gamma \rightarrow c\bar{c}$ , we have determined the parameters  $C_n, \beta_\gamma, s_0$  defined in (24). For Solutions I and II, they are as follows (in GeV units):

Solution I	Solution II	
$C_1 = -4.945$	$C_1 = -4.995$	
$C_2 = -2.893$	$C_2 = -2.897$	
$C_3 = -2.191$	$C_3 = -2.179$	
$C_4 = -2.300$	$C_4 = -2.260$	
$C_5 = -4.264$	$C_5 = -4.368$	
$C_6 = -0.690$	$C_6 = -0.479$	
$b_\gamma = 0.14$	$b_\gamma = 0.15$	
$s_0 = 11.9$	$s_0 = 22.5$	(38)

Experimental values of partial widths included into fitting procedure versus those obtained in the fitting procedure are shown in Table 4. There are also predictions made for the two-photon decays of the first radial excitation states:  $\eta_c(3594)$ ,  $\chi_0(3847)$ ,  $\chi_2(3947)$ .

Let us note that the decay  $\chi_{c2}(3556) \rightarrow \gamma\gamma$  was not included into the fit because of controversy of the data. In the reaction  $p\bar{p} \rightarrow \gamma\gamma$ , the value  $\Gamma(\chi_2(3556) \rightarrow \gamma\gamma) = 0.32 \pm 0.080 \pm 0.055$  keV was obtained [27], while in direct measurements, such as  $e^+e^-$  annihilation, the width is much larger:  $1.02 \pm 0.40 \pm 0.17$  keV [24],  $1.76 \pm 0.47 \pm 0.40$  keV [25],  $1.08 \pm 0.30 \pm 0.26$  keV [26]. The compilation [21] provides the value close to that of [27]. The value found in our fit agrees with data reported by [24, 25, 26] and contradicts [27].

## 4 Conclusion

We have carried out the calculations of radiative transitions, where the  $c\bar{c}$  system participates, and compared the results with the experiment. The results are given in Table 5. In general, there is a good description of the data. Still, one should point to a disagreement for the following two cases:  $\psi(2S) \rightarrow \chi_{c1}(1P)\gamma$  and  $J/\psi \rightarrow \eta_c(1S)\gamma$ .

The calculation of partial width  $\psi(2S) \rightarrow \chi_{c1}(1P)\gamma$  provides us with a value twice as large as given in [28, 29]. Such a disagreement may be related to either presumably much higher experimental error [28, 29] or a specific behaviour of the wave function of  $\chi_{c1}(1P)$ , that was not accounted for in [4].

Another discrepancy has been observed for the width of the transition  $J/\psi \rightarrow \eta_c(1S)\gamma$ . This is an M1-transition, it is defined by the magnetic moment of the  $c$ -quark. One possibility to reduce the calculated value of  $J/\psi \rightarrow \eta_c(1S)\gamma$  consists in the increase of the  $c$ -quark mass, another one is to include into consideration anomalous magnetic moment of  $c$ -quark. The hypothesis of the existence of anomalous magnetic moment at light quarks was suggested

Table 4: Calculated partial widths for  $nS$  and  $nP$  states *versus* experimental data (bold mass numbers stand for the predicted states)

Decay	$\Gamma$ (keV)	$\Gamma_{exp}$ (keV)
$1S : J/\psi(3096) \rightarrow e^+e^-$	5.444 (I) 5.598 (II)	$5.40 \pm 0.22$
$2S : \psi(3686) \rightarrow e^+e^-$	2.151 (I) 2.210 (II)	$2.14 \pm 0.21$
$3S : \psi(4040) \rightarrow e^+e^-$	0.756 (I) 0.778 (II)	$0.75 \pm 0.15$
$4S : \psi(4415) \rightarrow e^+e^-$	0.462 (I) 0.498 (II)	$0.47 \pm 0.10$
$1S : \eta_c(2979) \rightarrow \gamma\gamma$	6.979 (I) 6.946 (II)	$7.0 \pm 1.0$
$2S : \eta_c(3594) \rightarrow \gamma\gamma$	1.968 (I) 1.034 (II)	—
$1P : \chi_{c0}(3415) \rightarrow \gamma\gamma$	2.572 (I) 2.440 (II)	$2.6 \pm 0.5$
$2P : \chi_{c0}(\mathbf{3849}) \rightarrow \gamma\gamma$	1.159 (I)	—
$3P : \chi_{c0}(\mathbf{3845}) \rightarrow \gamma\gamma$	1.021 (II)	—
$1P : \chi_{c2}(3556) \rightarrow \gamma\gamma$	1.195 (I) 1.155 (II)	—
$2P : \chi_{c2}(\mathbf{3950}) \rightarrow \gamma\gamma$	2.051 (I)	—
$3P : \chi_{c2}(\mathbf{3943}) \rightarrow \gamma\gamma$	1.934 (II)	—

Table 5: Comparison of experimental data (in keV units) with our results and calculations of other groups.

Decay	Data	results	LS(F)[10]	LS(C)[10]	RM(S)[11]	RM(V)[11]	NR[32]
$\psi(2S) \rightarrow \chi_{c0}(1P)\gamma$	$26 \pm 4$	22	31–47	26–31	31	32	19.4
$\psi(2S) \rightarrow \chi_{c1}(1P)\gamma$	$25 \pm 4$	59	58–49	63–50	36	48	34.8
$\psi(2S) \rightarrow \chi_{c2}(1P)\gamma$	$20 \pm 4$	19	48–47	51–49	60	35	29.3
$\psi(2S) \rightarrow \eta_c(1S)\gamma$	$0.8 \pm 0.2$	0.4	11–10	10–13	6	1.3	4.47
$\chi_{c0}(1P) \rightarrow J/\psi(1S)\gamma$	$165 \pm 50$	169	130–96	143–110	140	119	147
$\chi_{c1}(1P) \rightarrow J/\psi(1S)\gamma$	$295 \pm 90$	389	390–399	426–434	250	230	287
$\chi_{c2}(1P) \rightarrow J/\psi(1S)\gamma$	$390 \pm 120$	229	218–195	240–218	270	347	393
$J/\psi(1S) \rightarrow \eta_c(1S)\gamma$	$1.1 \pm 0.3$	4.1	1.7–1.3	1.7–1.4	3.35	2.66	1.21
$J/\psi(1S) \rightarrow e^+e^-$	$5.4 \pm 0.22$	5.44	5.26	5.26	8.05	9.21	12.2
$\psi(2S) \rightarrow e^+e^-$	$2.12 \pm 0.12$	2.15	2.8–2.5	2.9–2.7	4.30	5.87	4.63
$\psi(3S) \rightarrow e^+e^-$	$0.75 \pm 0.15$	0.76	2.0–1.6	2.1–1.8	3.05	4.81	3.20
$\psi(4S) \rightarrow e^+e^-$	$0.47 \pm 0.10$	0.46	1.4–1.0	1.6–1.3	2.16	3.95	2.41
$\eta_c(1S) \rightarrow \gamma\gamma$	$7.0 \pm 0.9$	6.98	6.2–6.3	6.2–6.5	4.2	3.8	19.1
$\chi_{c0}(1P) \rightarrow \gamma\gamma$	$2.6 \pm 0.5$	2.57	1.6–1.8	1.5–1.6	–	–	–
$\chi_{c2}(1P) \rightarrow \gamma\gamma$	$1.02 \pm 0.40 \pm 0.17$ [24] $1.76 \pm 0.47 \pm 0.40$ [25] $1.08 \pm 0.30 \pm 0.26$ [26] $0.33 \pm 0.08 \pm 0.06$ [27]	1.17	0.3–0.4	0.3–0.4	–	–	–

rather long ago in connection with the description of the decay  $\omega \rightarrow \pi^0\gamma$  [30], see also discussion in [31].

In Table 5, the values of partial width are presented obtained by the other authors.

In [10], the ideology of treating the  $c\bar{c}$  system is similar to ours: the charmonium masses were fitted as well as the widths of radiative transitions. The results obtained in [10] depend on a chosen gauge for gluon exchange interaction — we demonstrate the results obtained both for Feynman (F) and Coulomb (C) gauges; different approaches used in [10] are reflected in the allowed accuracy intervals given in Table 5.

In [11] the  $c\bar{c}$  system was studied in terms of scalar (S) and vector (V) confinement forces — both variants are presented in Table 5. For the comparison we give in Table 5 the results obtained in the nonrelativistic approach to the  $c\bar{c}$  system.

Both in relativistic [10, 11] and nonrelativistic [32] approaches there is rather large discrepancy between the data and calculated values of  $\psi(nS) \rightarrow e^+e^-$  (in [10] the width of the transition  $J/\psi \rightarrow e^+e^-$  was not calculated but fixed). In our opinion, the reason is that in all above-mentioned papers, soft interaction of quarks was not accounted for — we mean the processes shown in Fig. 3b,c. In fact the necessity of taking into consideration the low-energy quark interaction, that is, the vector meson dominance in the transitions  $q\bar{q} \rightarrow V \rightarrow \gamma$ , was understood decades ago but till now this procedure has not become commonly accepted even for light quarks: see, for example, [33, 34].

## Acknowledgments

We thank A.V. Anisovich, Y.I. Azimov, G.S. Danilov, I.T. Dyatlov, L.N. Lipatov, V.Y. Petrov, H.R. Petry and M.G. Ryskin for useful discussions.

This work was supported by the Russian Foundation for Basic Research, project no. 04-02-17091.

## References

- [1] V.V. Anisovich, D.I. Melikhov, V.A. Nikonov, Phys. Rev. D**55**, 2918 (1997).
- [2] A.V. Anisovich, V.V. Anisovich, L.G. Dakhno, V.A. Nikonov, and A.V. Sarantsev, "Determination of quark–antiquark component of the photon wave function for  $u, d, s$  quarks", Yad. Fiz., in press; hep-ph/0406320, (2004).
- [3] O.V. Zenin, V.V. Ezhela, S.B. Lugovsky et al., Report IHEP-2001-25, hep-ph/0110176.
- [4] V.V. Anisovich, V.N. Markov, V.A. Nikonov, A.V. Sarantsev, "Energy levels and quark wave functions for  $c\bar{c}$  and  $b\bar{b}$  systems in terms of the spectral integral Bethe–Salpeter equation", in preparation.
- [5] A.V. Anisovich, V.V. Anisovich, B.N. Markov, M.A. Matveev and A. V. Sarantsev, Yad. Fiz. **67**, 794 (2004) [Phys. of Atomic Nuclei, **67**, 773 (2004)].
- [6] G. Hulth and H. Snellman, Phys. Rev D**24**, 2978 (1981).
- [7] S. Godfrey and N. Isgur, Phys. Rev. D**32**, 189 (1985).
- [8] S.N. Gupta, S.F. Radford and W.W. Repko, Phys. Rev. D**31**, 160 (1985).
- [9] W. Lucha, F. Schöberl, and D. Gromes, Phys. Rep. **200**, 127 (1991).
- [10] J. Linde and H. Snellman, Nucl. Phys. **A619**, 346 (1997).
- [11] J. Resag and C.R. Münz, Nucl. Phys. **A590**, 735 (1995).
- [12] P.C. Tiemejer and J.A. Tjon, Phys. Rev. **C49**, 494 (1994).
- [13] H. Hersbach, Phys. Rev. **C50**, 2562 (1994).
- [14] A.V. Anisovich, V.V. Anisovich, V.N. Markov, M.A. Matveev and A.V. Sarantsev, J. Phys. G: Nucl. Part. Phys. **28**, 15 (2002).
- [15] J.J. Hernandez, S. Navas and C. Patrignani, Phys. Rev. D**66**, 010001-730 (2002).
- [16] G. t'Hooft, Phys. Rev. D**14**, 3432 (1976).

- [17] A.V. Anisovich, V.V. Anisovich and V.A. Nikonov, Eur. Phys. J. A**12** 103 (2001).
- [18] A.V. Anisovich, V.V. Anisovich, V.N. Markov and V.A. Nikonov, Yad. Fiz. **65**, 523 (2002) [Phys. Atom. Nucl. **65**, 497 (2002)].
- [19] A.V. Anisovich, V.V. Anisovich, M.A. Matveev and V.A. Nikonov, Yad. Fiz. **66**, 946 (2003) [Phys. Atom. Nucl. **66**, 914 (2003)].
- [20] H. Hertsbach, Phys. Rev. **A46**, 3657 (1992).
- [21] K. Hagiwara et al. (PDG), Phys. Rev. D**66** 010001-1 (2002).
- [22] F. Gross and J. Milana, Phys. Rev. **D43**, 2401 (1991).
- [23] K.M. Maung, D.E. Kahana and J.W. Ng, Phys. Rev. **A46**, 3657 (1992).
- [24] M. Acciari et al., Phys. Lett. **B453**, 73 (1999).
- [25] K. Ackerstaff et al., Phys. Lett. **B439**, 197 (1998).
- [26] J. Dominick et al., Phys. Rev. **D50**, 4265 (1994).
- [27] T.A. Armstrong et al., Phys. Rev. Lett. **70**, 2988 (1993).
- [28] J. Gaiser et al., Phys. Rev. **D34**, 711 (1986).
- [29] C.J. Biddick et al., Phys. Rev. Lett. **38**, 1324 (1977).
- [30] I.G. Aznauryan and N. Ter-Isaakyan, Yad. Phys. **31**, 1680 (1980) [Sov. J. Nucl. Phys. **31**, 871 (1980)].
- [31] S.B. Gerasimov, hep-ph/0208049; FHD Proceedings, March 2002, Kobe University, Japan.
- [32] M. Beyer, U. Bohn, M.G. Huber, B.C. Metsch and J. Resag, Z.Phys **C55**, 307 (1992).
- [33] M.A. DeWitt, H.M. Choi and C.R. Ji, Phys. Rev. D**68**: 054026 (2003).
- [34] B.-W. Xiao, B.-Q. Ma, Phys. Rev. D **68**, 034020 (2003).

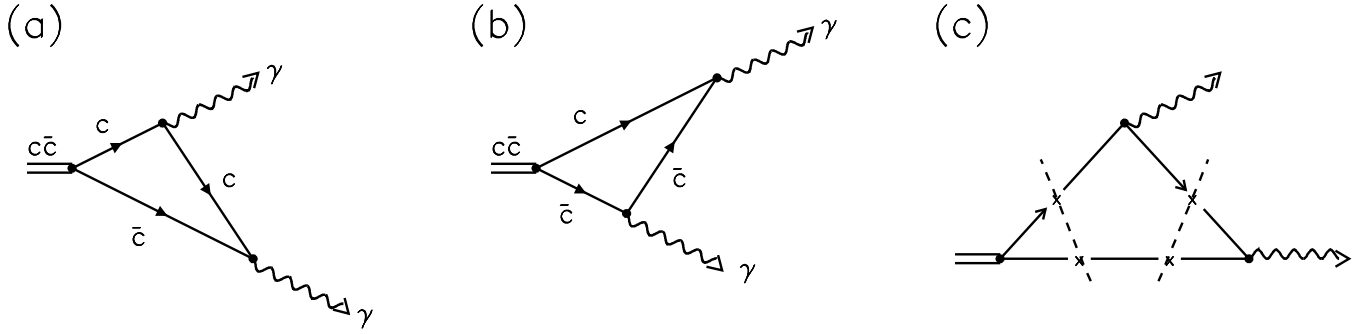


Figure 1: a,b) Diagrams for the two-photon decay of  $c\bar{c}$  state, c) Cuttings in the spectral integral representation.

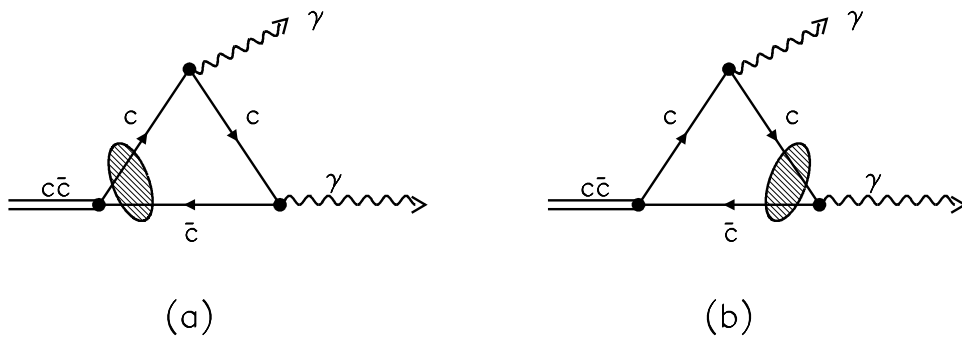


Figure 2: Initial (a) and final (b) state interactions of quarks in the decay diagrams.

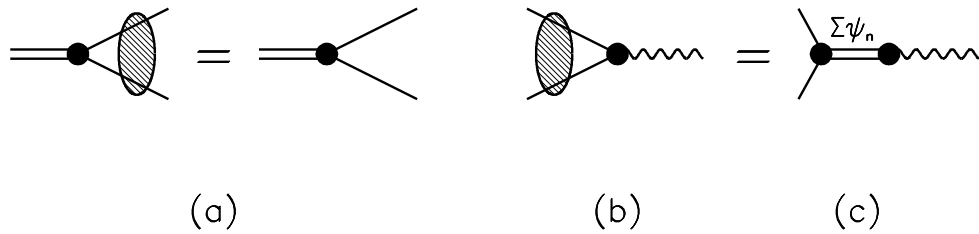


Figure 3: a) Graphical representation of the Bethe-Salpeter equation for the  $c\bar{c}$  vertex; c,d) interaction of quarks in the vertex  $c\bar{c} \rightarrow \gamma$  and its approximation by the sum of transitions  $c\bar{c} \rightarrow \Sigma\psi(nS) \rightarrow \gamma$ .



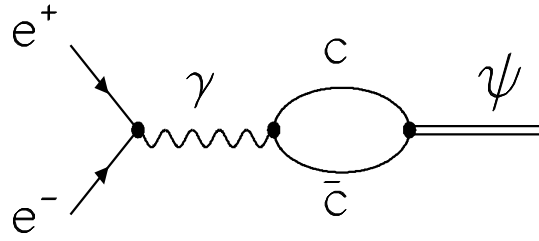


Figure 4: Quark transition diagram for the process  $e^+e^- \rightarrow \psi$ .

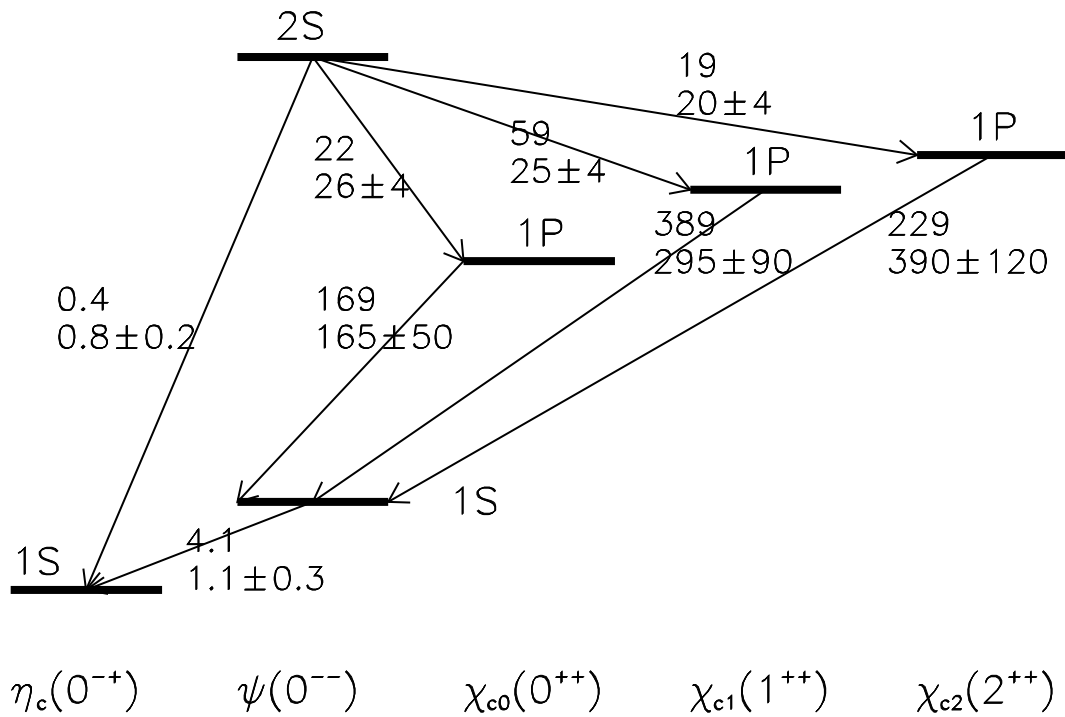


Figure 5: Radiative decays of the charmonium systems, which were taken into account in the fit [4]. The calculated decay partial widths are shown in the keV units (upper numbers) together with experimental data and errors accepted in the fit (lower numbers).

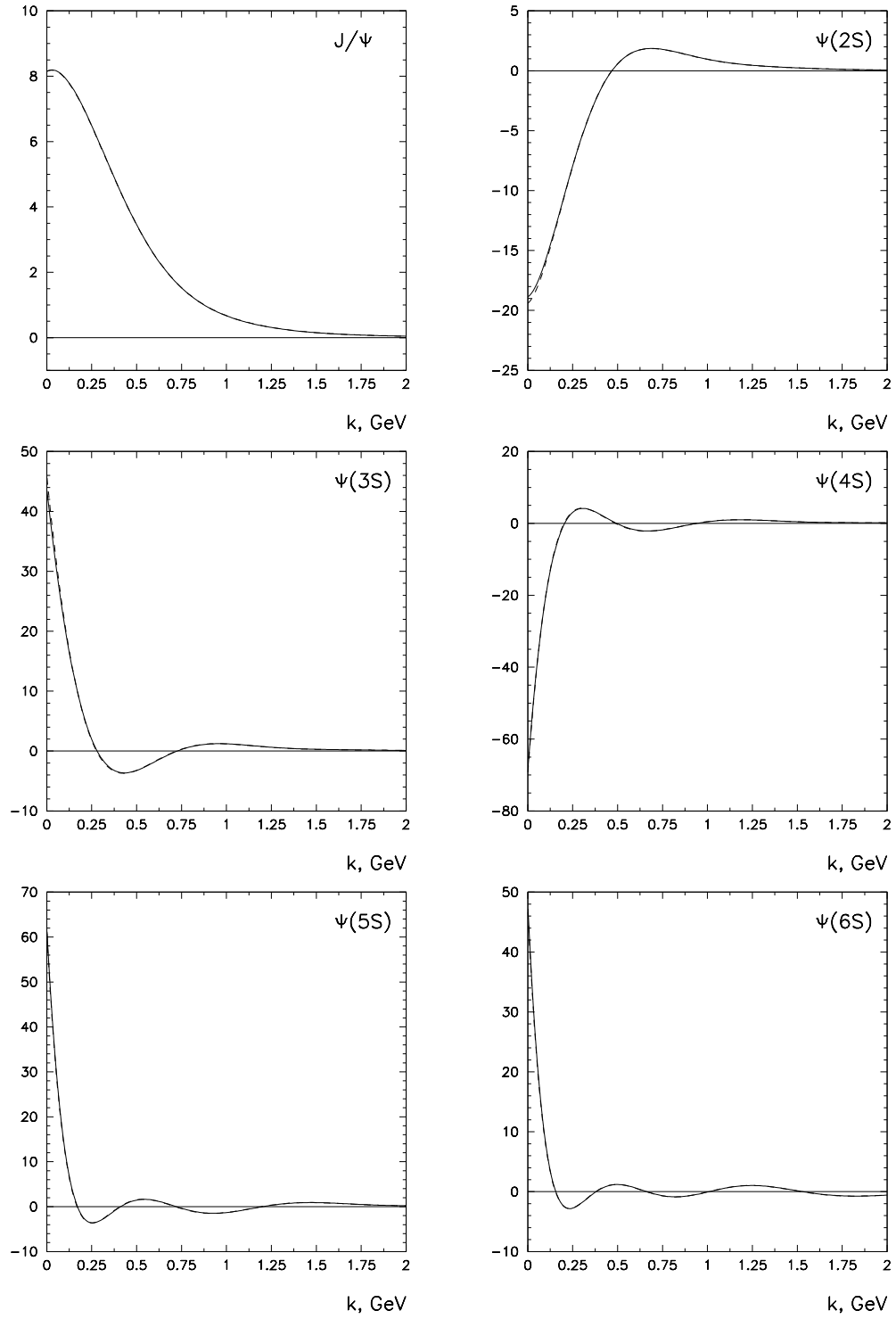


Figure 6: The  $c\bar{c}$  wave functions for  $\psi(nS)$ . Solid and dashed lines stand for Solutions I and II.

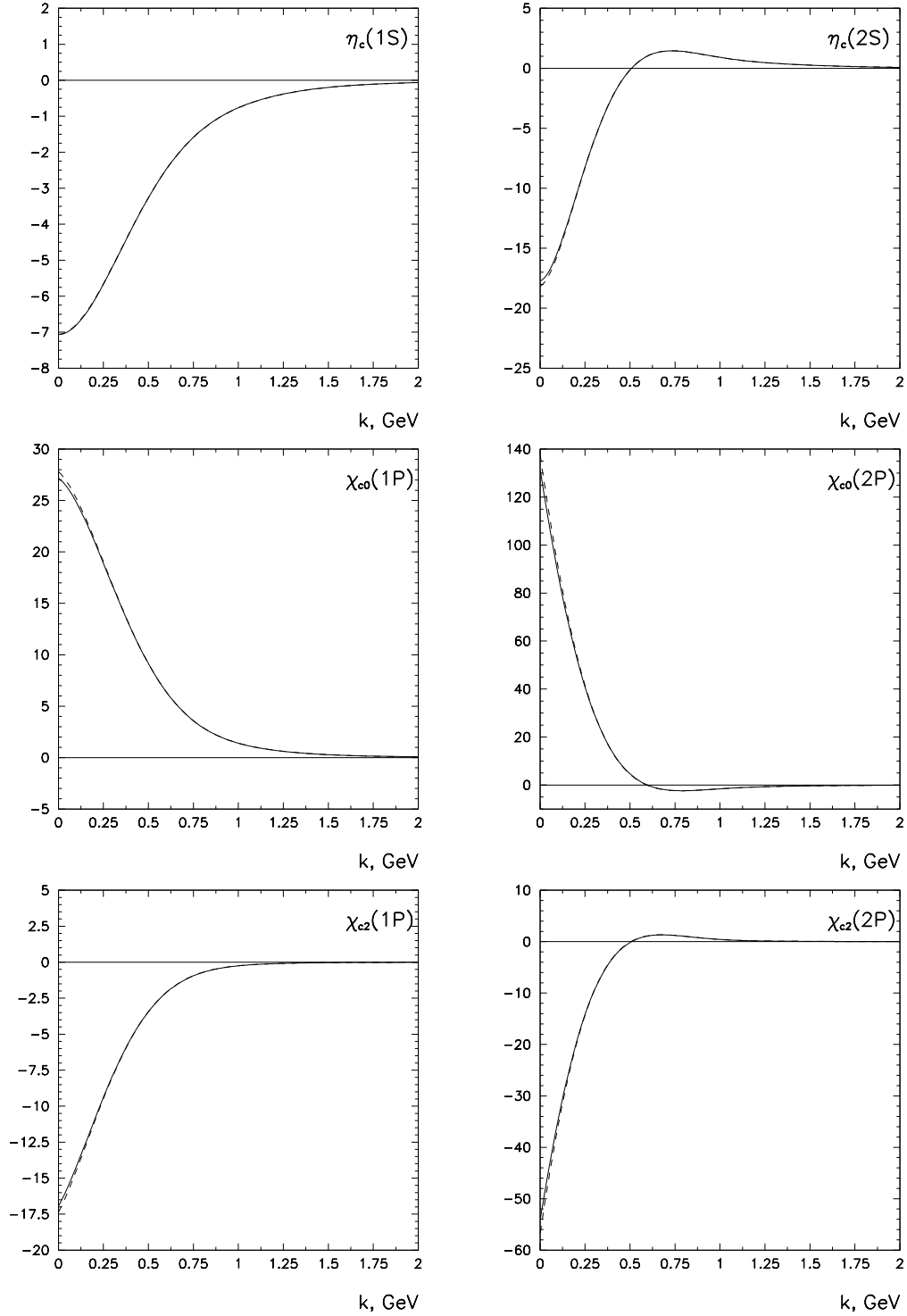


Figure 7: The  $c\bar{c}$  wave functions for  $\eta_c(nS)$ ,  $\chi_{c0}(nP)$  and  $\chi_{c2}(nP)$ . Solid and dashed lines correspond to Solutions I and II.

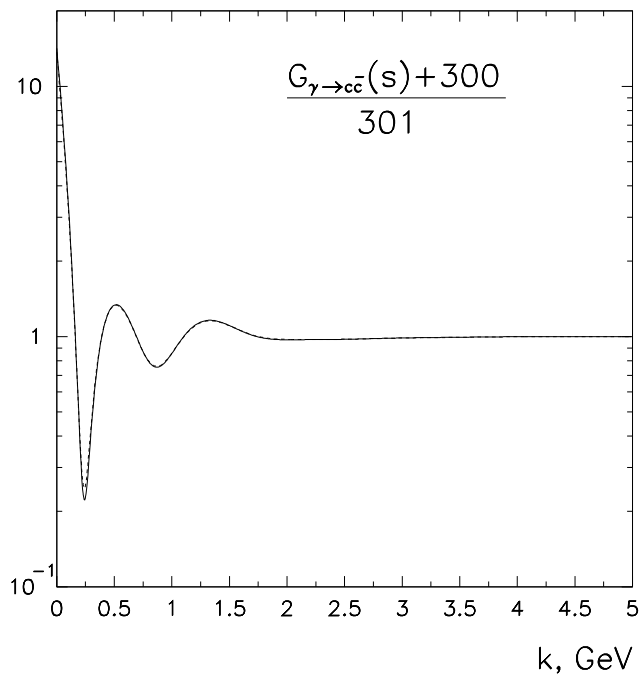


Figure 8: Vertex  $\gamma \rightarrow c\bar{c}$  ; solid and dashed lines correspond to Solutions I and II.

